The Role of Specific Amino Acid Residues in the Active Site of *Escherichia coli* DNA Polymerase I on Translesion DNA Synthesis Across from and Past an *N*-2-Aminofluorene Adduct†

Samer Lone‡ and Louis J. Romano*

Department of Chemistry, Wayne State University, Detroit, Michigan 48202

Received June 30, 2006; Revised Manuscript Received November 30, 2006

ABSTRACT: Understanding how carcinogenic DNA adducts compromise accurate DNA replication is an important goal in cancer research. A central part of these studies is to determine the molecular mechanism that allows a DNA polymerase to incorporate a nucleotide across from and past a bulky adduct in a DNA template. To address the importance of polymerase architecture on replication across from this type of bulky DNA adduct, three active-site mutants of *Escherichia coli* DNA polymerase I (Klenow fragment) were used to study DNA synthesis on DNA modified with the carcinogen *N*-2-aminofluorene (AF). Running-start synthesis studies showed that full-length synthesis past the AF adduct was inhibited for all of the mutants, but that this inhibition was substantially less for the F762A mutant. Single nucleotide extension and steady-state kinetic experiments showed that the Y766S mutant displayed higher rates of insertion of each incorrect nucleotide relative to WT across from the dG−AF adduct. This effect was not observed for F762A or E710A mutants. Similar experiments that measured synthesis one nucleotide past the dG−AF adduct revealed an enhanced preference by the F762A mutant for dG opposite the T at this position. Finally, synthesis at the +1 and +2 positions was inhibited to a greater extent for the Y766S and E710A mutants compared with both the WT and F762A mutants. Taken together, this work is consistent with the model that polymerase geometry plays a crucial role in both the insertion and extension steps during replication across from bulky DNA lesions.

Cellular DNA is under constant exposure to both endogenous and exogenous agents that are able to form covalently bound adducts. If unrepaired, these lesions can cause mutations by interfering with the accurate replication of the DNA across from or near the damaged site. Bulky lesions such as thymine dimers, polycyclic aromatic hydrocarbons, or aromatic amines are known to present a strong block to most A family, high fidelity polymerases. Alternatively, the Y family, bypass polymerases are able to synthesize past such damage, although sometimes with reduced fidelity (*1*). Compared to high fidelity DNA polymerases, the bypass polymerases have a much more open active site and for this reason make fewer contacts with the DNA template. A logical conclusion from these structural studies is that this open structure geometry enables these polymerases to more efficiently transverse a DNA lesion.

The mechanism by which a DNA polymerase achieves its remarkable accuracy has been the subject of intense study (*2*−*4*). Several lines of evidence suggest that nucleotide selection is primarily achieved through the geometrical constraints within the polymerase active site that allow the formation of correct Watson−Crick base pairs and reject base pairs that are not geometrically equivalent. Kinetic and structural studies have shown that the polymerase undergoes a conformational change upon the binding of the correct nucleotide, and this rearrangement is thought to deliver the incoming nucleotide to the polymerase active site and align it properly for nucleophilic attack by the 3′-hydroxyl of the primer (*5*). Apparently all high fidelity polymerases are able to reach a fully active catalytic configuration if the nucleotide can adopt a Watson−Crick geometry, and it is thought that this so-called induced-fit mechanism provides the selectivity during nucleotide incorporation.

Structural studies of the Pol A family of polymerases have shown that the conformational change from an open to closed structure that occurs upon binding of the correct nucleotide results in a sizable movement of the O helix in the fingers domain to generate a binding pocket that encompasses the incoming dNTP and the complementary template base (*5*). Several conserved residues within the polymerase binding pocket have important interactions with the incoming dNTP or the template-primer and have been shown to affect polymerase fidelity (*6*). For example, in the Klenow fragment of *E. coli* DNA polymerase I (KF)[1] substitutions of alanine or serine for the tyrosine at position 766 (Figure 1), an integral part of the O helix that has previously been shown

† This investigation was supported by Public Health Service Grant CA40605 awarded by the Department of Health and Human Services.

* Corresponding author. Tel: 313-577-2584. Fax: 313-577-8822. E-mail: LJR@chem.wayne.edu.

‡ Present address: Department of Physiology and Biophysics, Mount Sinai School of Medicine, New York, NY.

[1] Abbreviations: KF, Klenow fragment; WT, wild-type; dG−AAF, *N*-(2′-deoxyguanosin-8-yl)-2-acetylaminofluorene; dG−AF, *N*-(2′-deoxyguanosin-8-yl)-2-aminofluorene; AAF, *N*-2-acetylaminofluorene; AF, *N*-2-aminofluorene; PAGE, polyacrylamide gel electrophoresis; K_m, Michaelis constant; V_{max}, the maximum rate of reaction; F_{ins}, frequency of insertion; F_{ext}, frequency of extension.

10.1021/bi061324o CCC: $37.00
Published on Web 02/17/2007

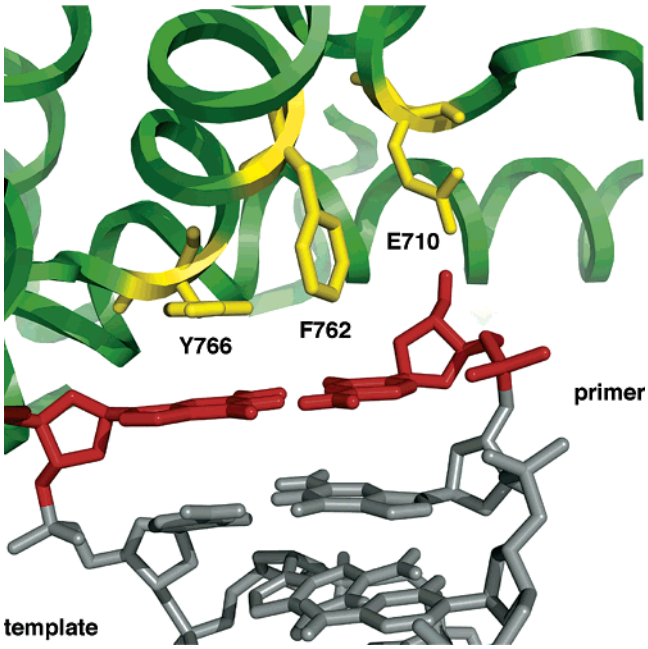

FIGURE 1: Representation of the positions of the Y766, F762, and E710 residues (polymerase I numbering) from the open structure of the Taq DNA polymerase I (*5*)

to be important in preserving the active site geometry within the base-pair binding pocket, resulted in a reduced fidelity for this mutant (*7*−*9*).

Another important residue located within the fingers domain is the phenylalanine located at position 762 (Figure 1). The phenyl ring of this residue has been described as a "paddling" device that sweeps incoming nucleotides into the binding pocket (*10*). Cocrystal structural information shows the phenyl ring stacking against the ribose portion of the incoming nucleotide (*5*). Biochemical data suggests that this residue positions the 3′-OH of the sugar for contact with an as yet unconfirmed H-bond acceptor. Without this essential contact, mutant KF polymerases with substitutions at this site have higher frequencies of insertion of dideoxy nucleotides (*10*). Unlike many other residues whose mutants have altered DNA fidelity on unmodified templates, the Phe-762 mutants have no apparent decrease in selectivity, relative to the wild-type (WT), for the correct nucleotide (*9*).

A third residue that has been shown to contribute to the proper polymerase active site conformation is Glu-710 (Figure 1), which is located in the so-called palm domain of KF. This residue has been thought to act as a "steric gate" that prevents ribonucleotide incorporation since replacement with a smaller alanine residue leads to increased rates of ribonucleotide incorporation (*11*). In addition to preventing ribonucleotide incorporation, the Glu-710 is also involved in nucleotide selectivity as the E710A mutant show an increased rate of misinsertions of purine nucleotides, but a decreased rate of misinsertions of pyrimidine nucleotides (*12*).

Recently, structures of the *E. coli* DNA polymerase I homologues, T7 DNA polymerase and *Bacillus* DNA polymerase I, complexed with *N*-(deoxyguanosin-8-yl)-2-(acetylamino)fluorene (dG−AAF) and *N*-(deoxyguanosin-8-yl)-2-aminofluorene (dG−AF) have been elucidated (*13*, *14*). These two bulky carcinogenic adducts (Figure 2) adopt very different structures in duplex DNA, and it is thought that

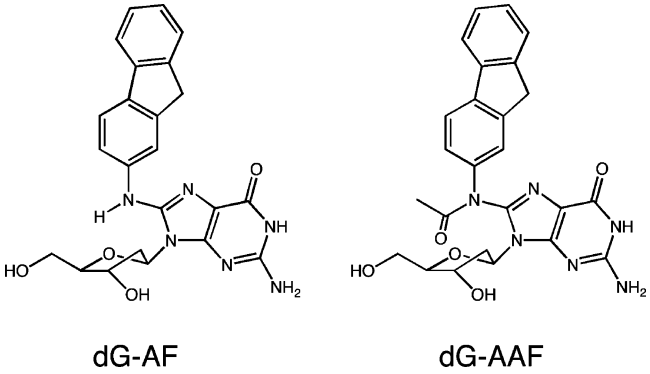

FIGURE 2: Structure of the dG−AF and dG−AAF adducts.

differences in their biological properties are related to these structural differences. Most spectral, enzymatic, and theoretical studies suggest that the *N*-2-aminofluorene (AF) structure, which represents the major adduct in many tissues (*15*), produces much less distortion in the DNA helix than the closely related *N*-2-acetylaminofluorene (AAF) adduct (*16*−*21*). The mutagenic consequences of each adduct are also quite distinct: while the dG−AAF adduct results in predominantly frameshift mutations in bacteria, the dG−AF adduct produces mostly base substitution mutations (*22*−*24*).

In the T7 DNA polymerase structure, the dG−AAF adduct adopts a syn conformation that facilitates the intercalation of its fluorene ring into a hydrophobic pocket on the surface of the fingers subdomain and locks the fingers in an open, inactive conformation (*13*). The intercalation of the fluorene rings distorts the helix such that the Y766 (polymerase I numbering) at the base of the helix is displaced into the nucleotide binding pocket, presumably preventing nucleotide incorporation by blocking nucleotide binding. The *Bacillus* DNA polymerase I structure indicates that the guanine bound to the AF adduct adopts a conformation similar to an unmodified base allowing it to form a base pair with the template base; however, the structure also reveals distortions in the C:dG−AF base pair that presumably slows synthesis past the adduct position (*14*). Taken together, these structures provide a molecular basis for the observed effects of these DNA adducts on replication and reveal a correspondence between the structures of the adducts in the polymerase active site and those in the duplex DNA.

To address the effect of active site geometry on translesion synthesis, we have examined how specific amino acid substitutions in the active site of *E. coli* DNA polymerase I (Klenow fragment) effect synthesis on and interactions with AAF and AF-modified primer-templates. Previously, we reported the role that tyrosine at position 766 plays in replication across from an AAF adduct (*25*). Consistent with the mechanistic importance of this residue, we observed that replacing the tyrosine with a smaller serine residue allowed the polymerase to incorporate nucleotides more readily across from a dG−AAF adduct. In the present study, we extend the studies with this mutant to the dG−AF adduct. In addition to examining the Tyr-766 residue, we also analyze the role of the Phe-762 and the Glu-710 residues and provide further insights into the structural basis for replicating across from and past this lesion.

MATERIALS AND METHODS

Materials. Wild-type Klenow fragment (exo$^-$) Y766S, F762A, and E710A mutant clones were generously provided by Dr. Catherine Joyce of Yale University. Both WT and mutant proteins were overexpressed and purified as described (*26*) and contained the D424A mutation, which eliminates the 3′−5′ exonuclease activity. The specific activity of the protein was determined as described (*27*). Protein concentrations were determined by colorimetry using a Bradford assay (*28*) employing Bio-Rad reagents. T4 polynucleotide kinase was purchased from Amersham Pharmacia Biotech. dNTPs were purchased from Amersham Pharmacia Biotech. [γ-^{32}P]-ATP was from ICN Biomedicals. *N*-Acetoxy-2-acetylaminofluorene was obtained from the NCI Chemical Carcinogen Reference Standard Repository.

Synthesis and Purification of Oligonucleotides. All oligonucleotides were purified by denaturing polyacrylamide gel electrophoresis. Site-specifically modified 28-mer templates were synthesized, purified, and characterized, as described (*29*).

Primer Extension Analysis: Running-Start. ^{32}P-labeled 12-mer primer (1 nM) was annealed to a 2-fold excess of the AF-modified 28-mer template (5-GTGATG$^{(AF)}$ ATAAGTG-GCCGTCGTTTTCGTC-3′) by heating to 90 °C and slow cooling. This mixture was added to a solution of dNTPs (100 μM) in 50 mM Tris-HCl, pH 7.5, containing 10 mM $MgCl_2$, 1 mM dithiothreitol, and 0.05 mg/mL bovine serum albumin. The reaction (final volume 100 μL) was initiated by the addition of 0.5 pmol of KF, and the mixture was incubated at room temperature for the indicated times (0−15 min). Aliquots (10 μL) of the reaction mixture were removed, and synthesis was stopped by cooling to 0 °C and the addition of 10 μL of gel loading buffer, which contained 90% formamide and 5 mg/mL bromophenol blue and xylene cyanol. The samples were analyzed on a 20% denaturing polyacrylamide gel, and product formation was measured with a Molecular Dynamics Storm 860 phosphoimager using ImageQuant for quantification. Total bypass synthesis was determined by dividing the total radioactivity past the adduct at each time point by the total radioactivity in each lane. Full extension was determined by dividing the total radioactivity of the 28-mer product by the total radioactivity in each lane.

Primer Extension Analysis: Standing-Start. ^{32}P-labeled primers (1 nM) were annealed to a 2-fold excess of the AF-modified 28-mer template by heating to 90 °C and slow cooling. This mixture was added to a solution containing 50 mM Tris-HCl, pH 7.5, 10 mM $MgCl_2$, 1 mM dithiothreitol, 0.05 mg/mL bovine serum albumin, and either all four dNTPs or an individual dNTP (100 μM). The reaction (final volume 10 μL) was initiated by the addition of 0.02 pmol of KF, and the mixture was incubated at room temperature for 10 min. Synthesis was stopped by the addition of 10 μL of gel loading buffer containing 90% formamide, 5 mg/mL of both bromophenol blue and xylene cyanol. An aliquot was analyzed on a 20% denaturing polyacrylamide gel, and product formation was measured by phosphoimager analysis. Total bypass synthesis was determined by dividing the total radioactivity across from and extending past the adduct by the total radioactivity in each lane. Single nucleotide extension was determined by dividing the total radioactivity of the insertion product by the total radioactivity in each lane.

Steady-State Kinetics. Steady-state kinetics using standing-start single nucleotide insertion and extension reactions were carried out similar to those described in ref *30*. Typical reactions were carried out in 10 μL volumes in the presence of 50 mM Tris-HCl, pH 7.5, 10 mM $MgCl_2$, 1 mM dithiothreitol, and 0.05 mg/mL bovine serum albumin. Primer-templates (final concentration 0.1 μM) were annealed by heating to 90° and slow cooling. Reactions were initiated by the addition of 0.01 to 0.1 pmol of DNA polymerase and were incubated at room temperature for 1 to 12 min at dNTP concentrations ranging from 0.020 to 500 μM. Both polymerase concentrations and times were varied for each nucleotide examined to ensure that less than 20% incorporation occurred. The extent of each reaction was determined by running reaction samples that had been quenched by the addition of 95% formamide, 20 mM EDTA, 0.05% xylene cylanol and bromophenol blue, on a 20% denaturing polyacrylamide gel to separate unreacted primer from insertion products. Relative velocities were calculated as described previously (*31*) by dividing the extent of the reaction by the reaction time and normalized for the varying enzyme concentrations that were used. The Michaelis constant (K_m) and maximum rate of the reaction (V_{max}) were obtained from Hanes−Wolf plots of the kinetic data. Insertion (F_{ins}) and extension (F_{ext}) frequencies were determined relative to dC:dG and dA:dT, respectively, according to equations developed by Mendelman (*32*, *33*). The frequency of insertion and extension are defined as $F = (V_{max}/K_m)[\text{wrong pair}]/(V_{max}/K_m)[\text{correct pair}]$. All reactions reported represent an average of at least three experiments and had standard deviations less than 20%.

RESULTS

Primer Extensions Using the AF-Modified Templates. Replication was first examined for both the WT and mutant KF polymerases using a running start primer-extension reaction (Figure 3). Replication by the WT polymerase on the AF-modified primer-template, shown in Figure 3A, provided approximately 80% synthesis past the dG−AF adduct over the 15 min time course, with minor stalling directly across from and near the adduct, especially in the early time points of the reaction (Figures 3B and 3C). Each of the KF mutant polymerases displayed a different pattern of replication products (Figure 3B). With the Y766S mutant polymerase, synthesis was severely blocked at the dG−AF adduct site, showing approximately 25% extension past the adduct and less than 5% formation of the full 28-mer product after 15 min (Figure 3C). The F762A mutant also showed substantial stalling at the adduct site; however after 15 min synthesis past the adduct was greater (62%) than was observed with the Y766S mutant. Finally, the E710A mutant was almost completely blocked at the adduct site with less than 20% extension past the adduct and less than 2% full extension product (Figure 3C).

Standing-Start Primer Extension at the Adduct Site. Single nucleotide extension analysis was performed to qualitatively determine the nucleotide specificity for the mutant polymerases across from the dG−AF adduct. Using the 22/28 primer-templates shown in Figure 4A, insertion was measured directly across from the adduct using each of the four individual nucleotides for each of the KF polymerases (Figure 4B). Under these enzyme excess conditions, all four

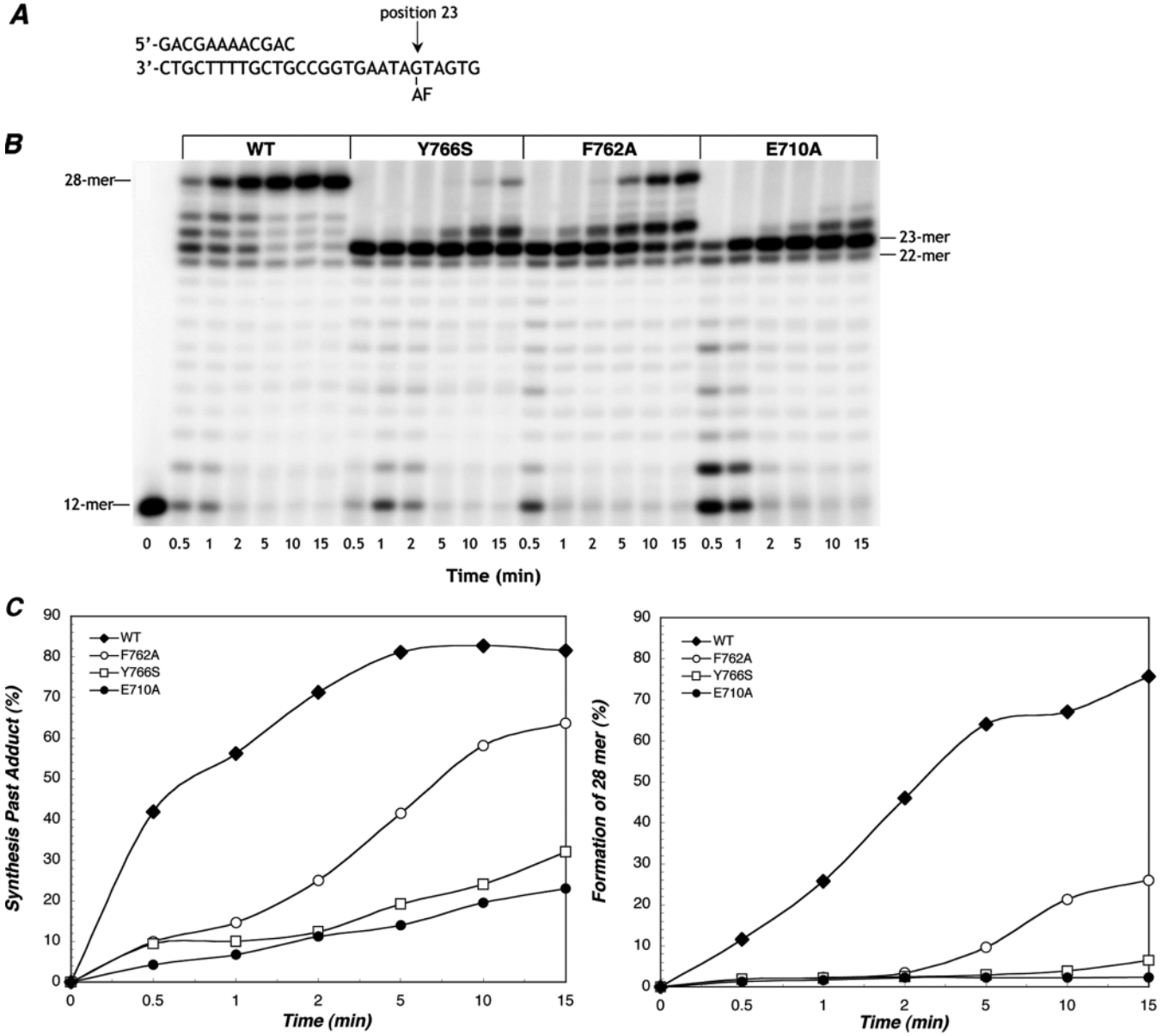

FIGURE 3: Running-start primer extension analysis of AF-modified primer-templates. (A) The indicated 12-mer primer was annealed to the 28-mer template containing an dG−AF adduct at the position indicated. (B) Synthesis was carried out by both the WT and mutant Klenow fragments (exo$^-$) as described in "Materials and Methods". The final concentrations in the reaction mixture were 1 nM primer-template, 5 nM polymerase, 100 μM dNTPs, 50 mM Tris-HCl, pH 7.5, 10 mM $MgCl_2$, 1 mM dithiothreitol, and 0.05 mg/mL bovine serum albumin. Each reaction was terminated after the period of time indicated under each lane. (C) The amount of extension past the adduct (left panel) and the amount of fully extended 28-mer product (right panel) are representative of the experiment shown in panel B. The amount of extension was determined by phosphorimager analysis, and the levels were determined using Molecular Dynamics ImageQuant software.

polymerases exhibited preferential incorporation of dC across from the dG−AF adduct but the Y766S mutant was significantly less selective for correct nucleotide incorporation while the F762A and E710A mutants had similar selectivity compared to the WT enzyme.

Single Nucleotide Incorporation Kinetics at the Adduct Site. Steady-state kinetic analyses were performed to quantify more accurately the insertion frequencies for incorporation across from the dG−AF adduct by the mutant KF polymerases. In addition, incorporation of the correct nucleotide (dC) was measured on an undamaged primer-template having the same sequence (Table 1). As expected the WT polymerase was more efficient than each of the mutants at incorporation on undamaged DNA (Table 1). The ratio of the reaction rates (V_{max}/K_m) for incorporation of each of the individual nucleotides vs that for incorporating dC across undamaged DNA provides a nucleotide selectivity factor (F_{ins}). The F_{ins} for the individual nucleotides for each mutant can then be compared to that determined for the WT polymerase. When the AF modified primer-templates were used, each mutant showed decreased rates of insertion (V_{max}/K_m) for the correct nucleotide (Table 1), however when normalized for insertion across undamaged DNA each of the proteins showed relatively the same frequency of incorporation (F_{ins}) for correct nucleotide. Although dC was the preferred nucleotide for the Y766S mutant, this mutant displayed an enhanced ability to incorporate an incorrect nucleotide compared with WT KF. As shown in Table 1, the F_{ins} ratios (mutant/WT) for this mutant were 8.6, 10.2, and 113 for dG, dA, and dT, respectively. Interestingly, the

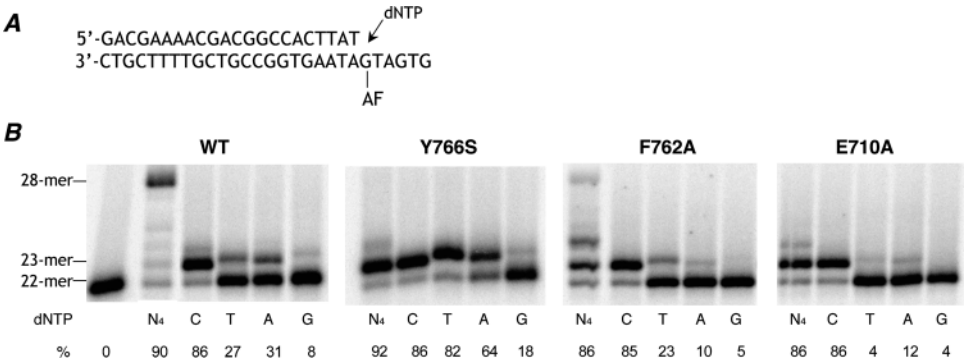

FIGURE 4: Single nucleotide primer extensions directly across from the AF-modified primer-templates. The 22-mer primer was annealed to the indicated AF-modified 28-mer template, and synthesis was carried out as described in "Materials and Methods". The final concentrations in the reaction mixture were 1 nM primer-template, 2 nM polymerase, 100 μM dNTPs, 50 mM Tris-HCl, pH 7.5, 10 mM $MgCl_2$, 1 mM dithiothreitol, and 0.05 mg/mL bovine serum albumin. The % incorporation is indicated under each lane and was determined by phosphorimager analysis using Molecular Dynamics ImageQuant software. N_4 refers to the presence of all four dNTPs.

Table 1: Kinetic Parameters for Insertion by WT and Mutant Klenow Fragments[a]

dNTP:X[b]	K_m	V_{max}	V_{max}/K_m (% min^{-1} μM^{-1})	F_{ins}[c]	$[F_{ins}$(mutant)]/$[F_{ins}$(WT)]
WT					
dCTP:dG	1.9	43	22.6	1	
dCTP:dG−AF	5.8	20	3.5	1.6×10^{-1}	
dGTP:dG−AF	8.1	2.6×10^{-2}	3.2×10^{-3}	1.4×10^{-4}	
dATP:dG−AF	12	1.3×10^{-1}	1.1×10^{-2}	4.9×10^{-4}	
dTTP:dG−AF	21	1.4×10^{-1}	6.7×10^{-3}	3.0×10^{-4}	
Y766S					
dCTP:dG	3.4	18	5.3	1	
dCTP:dG−AF	4	7.7	1.9	3.6×10^{-1}	2.3
dGTP:dG−AF	5.3	3.3×10^{-2}	6.2×10^{-3}	1.2×10^{-3}	8.6
dATP:dG−AF	4.5	1.2×10^{-1}	2.7×10^{-2}	5.1×10^{-3}	10.4
dTTP:dG−AF	12	2.2	1.8×10^{-1}	3.4×10^{-2}	113
F762A					
dCTP:dG	19	5.6	0.3	1	
dCTP:dG−AF	9.3	8.6×10^{-1}	9.3×10^{-2}	3.1×10^{-1}	1.9
dGTP:dG−AF	61	1.4×10^{-4}	2.3×10^{-6}	7.7×10^{-6}	5.5×10^{-2}
dATP:dG−AF	51	8.0×10^{-3}	1.6×10^{-4}	5.3×10^{-4}	1.1
dTTP:dG−AF	38	1.3×10^{-2}	3.4×10^{-4}	1.1×10^{-3}	3.7
E710A					
dCTP:dG	2.4	7.7	3.2	1	
dCTP:dG−AF	5.9	1.5	2.5×10^{-1}	7.8×10^{-2}	4.9×10^{-1}
dGTP:dG−AF	3.0	2.0×10^{-4}	6.7×10^{-5}	2.1×10^{-5}	1.5×10^{-1}
dATP:dG−AF	4.1	4.5×10^{-3}	1.1×10^{-3}	3.4×10^{-4}	6.9×10^{-1}
dTTP:dG−AF	8.6	5.3×10^{-3}	6.2×10^{-4}	1.9×10^{-4}	6.3×10^{-1}

[a] Kinetics of insertion were determined as described under Materials and Methods using the primer-template shown above. Final concentrations of reaction mixtures contained 1−10 nM KF protein and 100 nM primer-template. All values represent the mean of at least three experiments and have standard deviations <20%. [b] X corresponds to either an unmodified or AF-modified guanine. [c] Frequencies of nucleotide insertion were determined using the equation $F_{ins} = (V_{max}/K_m)$[dN:dG−AF]/(V_{max}/K_m)[dC:dG].

F762A mutant showed enhanced selectivity, compared with the WT polymerase, that reduced the incorporation of dG but similar selectivity for both dT and dA (Table 1), while the selectivity by the E710A mutant resembled the WT polymerase.

Primer Extensions Past the Adduct. Single nucleotide extension reactions were carried out with primers extending across from the adduct, to the +1 and +2 positions (Figures 5, 6, and 7) using the WT and each of the mutant KF polymerases. Using the primer that ends across from the adduct (Figure 5), experiments using excess levels of WT polymerase showed incorporation of primarily the correct nucleotide and significant amounts of incorporation of the incorrect nucleotides. Similar experiments with the Y766S and F762A mutants qualitatively indicated that these polymerases were more prone to incorporate a purine at this position while the E710A mutant was much more specific for incorporation of the correct nucleotide, dA, at this position (Figure 5). These qualitative results were confirmed for the F762A mutant using steady-state kinetic analysis (Table 2), which showed that the relative F_{ins} of the mutant compared with WT for incorporation of dG was 46-fold. It is intriguing that the F762A mutant was significantly less accurate at this position than it was for incorporation directly across from the dG−AF adduct.

Incorporation at the +2 and +3 positions was accurate for both the WT and mutant polymerases although both the WT and Y766S KF displayed an ability to incorporate some dC at the +2 position (Figure 6). Every other mutant displayed a strong preference for incorporation of the correct nucleotide at the +2 position, and all of the polymerases showed high preference for the correct nucleotide at the +3 position (Figures 6 and 7). Similar to the results seen at the +1 position, both WT and F762A KF showed large amounts

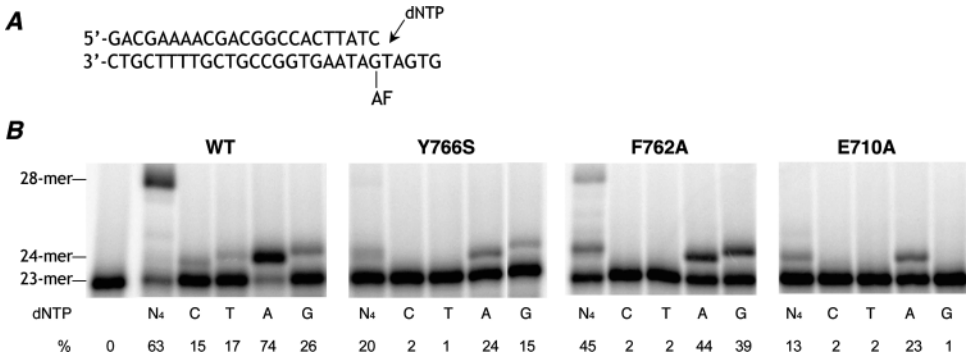

FIGURE 5: Single nucleotide primer extensions at the +1 position. The 23-mer primer was annealed to the indicated AF-modified 28-mer template, and synthesis was carried out as described in "Materials and Methods". The final concentrations in the reaction mixture were 1 nM primer-template, 2 nM polymerase, 100 μM dNTPs, 50 mM Tris-HCl, pH 7.5, 10 mM $MgCl_2$, 1 mM dithiothreitol, and 0.05 mg/mL bovine serum albumin. The % incorporation is indicated under each lane and was determined by phosphorimager analysis using Molecular Dynamics ImageQuant software. N_4 refers to the presence of all four dNTPs.

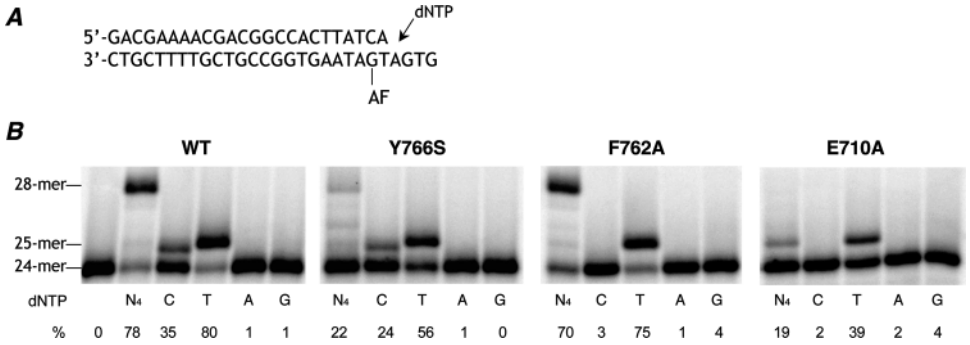

FIGURE 6: Single nucleotide primer extensions at the +2 position. The 24-mer primer was annealed to the indicated AF-modified 28-mer template, and synthesis was carried out as described in "Materials and Methods". The final concentrations in the reaction mixture were 1 nM primer-template, 2 nM polymerase, 100 μM dNTPs, 50 mM Tris-HCl, pH 7.5, 10 mM $MgCl_2$, 1 mM dithiothreitol, and 0.05 mg/mL bovine serum albumin. The % incorporation is indicated under each lane and was determined by phosphorimager analysis using Molecular Dynamics ImageQuant software. N_4 refers to the presence of all four dNTPs.

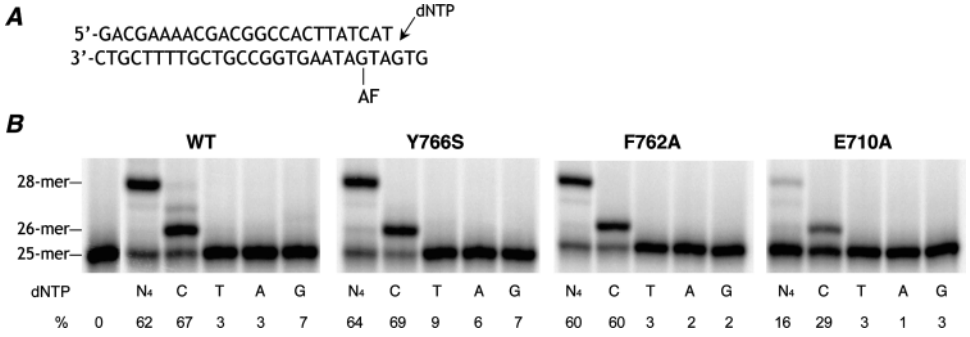

FIGURE 7: Single nucleotide primer extensions at the +3 position. The 25-mer primer was annealed to the indicated AF-modified 28-mer template, and synthesis was carried out as described in "Materials and Methods". The final concentrations of the reaction mixture were 1 nM primer-template, 2 nM polymerase, 100 μM dNTPs, 50 mM Tris-HCl, pH 7.5, 10 mM $MgCl_2$, 1 mM dithiothreitol, and 0.05 mg/mL bovine serum albumin. The % incorporation is indicated under each lane and was determined by phosphorimager analysis using Molecular Dynamics ImageQuant software. N_4 refers to the presence of all four dNTPs.

of full extension at the +2 position while the Y766S and E710A KF showed little to no full length extension (Figure 6). However, at the +3 position, the Y766S was able to overcome its reduced extension ability and like WT and F762A KF was able to reach significant amounts of full-length 28-mer product. Interestingly, at this position E710A mutant showed little full extension.

DISCUSSION

It is of considerable interest to understand how a DNA polymerase responds to the presence of DNA damage since permanent blockage of a replication fork could result in an apoptotic response, while misreading by a polymerase could lead to a potentially carcinogenic mutation. A well-studied type of DNA lesion is the damage induced in cells following exposure to the chemical carcinogen *N*-2-acetylaminofluorene. Three adducts are known to form, the closely related and well-studied C8-AAF−dG and C8-AF−dG as well as an adduct bound to the N2 position of guanine (*23*, *34*). Although the chemical structures of the two C8 adducts differ only by the presence of an acetyl group in the AAF structure, their conformations in DNA and biological effects are quite diverse (*19*, *20*). The dG−AAF adduct is one of the more distorting DNA adducts, presumably because the presence

Table 2: Kinetic Parameters for Insertion by WT and Mutant Klenow Fragments at the +1 Position[a]

dNTP	V_{max}/K_m (% min^{-1} μM^{-1})	F_{ins}[b]	[F_{ins}(mutant)]/[F_{ins}(WT)]
Unmodified Template			
WT			
dATP	10.4	1	
dGTP:dT	0.36	0.035	
F762A			
dATP	0.22	1	
dGTP	0.007	0.032	1
AF-Modified Template:			
WT			
dATP	11	1	
dGTP	0.12	0.011	
F762A			
dATP	0.08	1	
dGTP	0.04	0.5	46

[a] Kinetics of insertion were determined as described under Materials and Methods using the primer-template shown above. Final concentrations of reaction mixtures contained 1−10 nM KF protein and 100 nM primer-template. All values represent the mean of at least three experiments and have standard deviations <20%. [b] Frequencies of nucleotide insertion were determined using the equation $F_{ins} = (V_{max}/K_m)[dG:dT]/(V_{max}/K_m)[dA:dT]$.

of the acetyl group leads to a greater stability of the *syn* conformation in which the guanine has rotated around the glycosidic bond. This adduct presents a strong block to most high fidelity polymerases (*35*, *36*) and leads primarily to frameshift mutations in bacteria (*24*), which are likely formed via a looped out DNA structure in the polymerase active site (*37*, *38*). Alternatively, the AF lesion is one of the least distorting bulky DNA adducts, and this adduct can be relatively rapidly and accurately bypassed by most DNA polymerases. Thus, it is important to understand how these structural differences result in the observed different biological properties in general and specifically how each adduct affects the interactions between the amino acid residues in the polymerase active site and DNA template.

The process of translesion synthesis involves insertion of nucleotides opposite the lesion and extension from this position. Both steps are crucial for the efficient bypass of bulky DNA lesions. Structural studies with high fidelity polymerases reveal that, in addition to having interactions that form the binding pocket, DNA polymerases also interact extensively with the primer-template duplex (*39*). Chemical footprinting and fluorescence spectroscopy studies show that the polymerase domain of KF contacts five to eight base pairs of duplex DNA (*40*). Many of these are electrostatic interactions with the sugar−phosphate backbone of the DNA. Other contacts occur in the minor groove, including hydrophobic interactions and H-bonds between specific side chains and the N-3 atoms of purines and the O-2 atoms of pyrimidines (*6*). Taken together, these observations suggest that the polymerase plays an active role in checking the "correctness" of the active site before further extension.

Recently, structures of two A family polymerases complexed to primer-templates containing AAF and AF DNA lesions have been reported. The AAF moiety was found to intercalate into a hydrophobic pocket behind the O helix of the fingers subdomain causing this helix to move into a position that blocks the nucleotide binding site (*13*). In contrast, the structure containing the dG−AF adduct in the preinsertion complex shows the modified base in a *syn* conformation and the O helix remaining in an open conformation (*14*). In the postinsertion structure, the C:G-AF base pair causes significant distortion to the active site region with the modified base in a normal *anti* conformation and the AF lesion positioned in the major groove blocking the positioning of the next template base into the preinsertion site (*14*).

In the present study, the effect of positioning the dG−AF lesion in pre- and postinsertion sites was determined for the WT KF and three mutant polymerases known to have altered fidelity. As expected, the dG−AF adduct was not a strong block to synthesis at or past the adduct position for the WT polymerase. In this case the rate of nucleotide incorporation was reduced approximately 4-fold for incorporation across from the adduct compared with an unmodified template (Table 1), but the incorporation rate was about the same at the +1 position compared with an unmodified template (Table 2). Thus, although the crystal structure shows that the C:G-AF base pair distorts the active site region, this distortion apparently does not slow nucleotide incorporation.

The Y766S mutant (Figure 1) is known to have reduced fidelity, and the tyrosine at this position is thought to be important in preserving active site geometry within the base-pair binding pocket (*7*−*9*). Crystal structures of the homologous Taq polymerase in open and closed conformations indicate that, when the closed structure forms, this tyrosine rotates from a stacked position on top of the terminal template base pair to a position in front of the incoming nucleotide (*41*). Prior studies with the dG−AAF adduct using this mutant revealed enhanced incorporation at the adduct site but decreased extension past the lesion (*25*). The crystal structure suggests that the absence of this residue might allow room for dNTP binding even with the O helix moved forward by the dG−AAF adduct (*13*).

Synthesis by the Y766S mutant across from the dG−AF adduct was very efficient, with comparable rates of synthesis at this position compared to the WT polymerase (Figure 3B, Table 1). However the inhibition of synthesis for this mutant at the +1 position (Figure 3) was substantial, a result very similar to what is observed in the case of the dG−AAF adduct. In addition, the fidelity of nucleotide incorporation across from the dG−AF position was substantially reduced (compared with WT KF), with higher levels of dA and dG and substantially higher levels of dT being incorporated at this site (Table 1, Figure 4). Prior studies have shown that this mutant is less able to extend from a mispaired primer (*7*, *8*), and it is possible that the effect of the dG−AF adduct on incorporation is related to these results. Thus, the absence of this residue is thought to lead to an altered active site geometry resulting in a structure that is a poor substrate for incorporation of the next nucleotide (*7*, *8*). Since it has been shown that the dG−AF adduct causes a substantially altered geometry for the base pair located in the postinsertion site (*14*), it is possible that this distorted structure is exacerbated by the absence of this tyrosine, causing a strong blockage at this site. It is interesting to note that this mutation also leads to reduced accuracy and an inhibition of synthesis at the +2 position but not at the +3 position (Figures 6 and 7).

The E710A mutant displayed properties similar to the Y766S polymerase. The glutamic acid at this position has been shown to effect polymerase fidelity and, in addition,

this mutant displays much higher levels of ribonucleotide incorporation. Like the Y766S mutant, it is also inefficient at extension from a mispaired primer suggesting that it is less able to deal with a distortion at the 3′-end of the primer (*7*, *8*). Thus, like Y766S, this mutant allowed incorporation opposite the dG−AF adduct and extension past this position was essentially blocked.

Finally, of the three mutants studied, the F762A mutant was the least inhibited by the dG−AF adduct (Figure 3C), and this mutant does not display a reduced fidelity relative to the WT on unmodified templates (*9*). It is possible that a loss of the phenylalanine at this position does not alter the active site geometry in a way that alters the base pair orientation. However, although this mutant displays similar fidelity compared with the WT polymerase across from the dG−AF adduct, it is substantially less accurate at the +1 position, showing a strong preference to misincorporate dG across from the template dT.

The results presented in this study appear to indicate that there are different mechanisms at work for synthesis across from vs past an dG−AF adduct. Each of the mutant polymerases, which, based on the size of the amino acid changes, are likely to have a more open or loose active site, are able to incorporate across from the adduct but are moderately to greatly inhibited at positions one or two nucleotides past the adduct compared with the WT KF. Even though it is well-established that the Y family, bypass polymerases have a more open active site (*42*−*45*), there is biochemical and structural evidence that two polymerases may be necessary to bypass some bulky DNA adducts (*46*−*50*). In support of this mechanism, *in vitro* experiments show that pol ζ appears to be specialized at extending distorted primer-templates (*51*, *52*). One possible explanation for this two-step mechanism is that the open active site that is required for incorporation across from a bulky adduct does not constrain the distorted, modified base pair sufficiently to allow for synthesis at the +1 or +2 positions. The results presented here using KF mutants having more open and less constrained active sites support this model and, in addition, show that subtle differences within the polymerase active site allow for very different replication characteristics.

REFERENCES

1. Prakash, S., Johnson, R. E., and Prakash, L. (2005) Eukaryotic translesion synthesis DNA polymerases: specificity of structure and function, *Annu. Rev. Biochem. 74*, 317−353.
2. Goodman, M. F. (1997) Hydrogen bonding revisited: geometric selection as a principal determinant of DNA replication fidelity, *Proc. Natl. Acad. Sci. U.S.A. 94*, 10493−10495.
3. Johnson, K. A. (1993) Conformational coupling in DNA polymerase fidelity, *Annu. Rev. Biochem. 62*, 685−713.
4. Doublie, S., Sawaya, M. R., and Ellenberger, T. (1999) An open and closed case for all polymerases, *Structure Fold Des. 7*, R31−35.
5. Li, Y., Korolev, S., and Waksman, G. (1998) Crystal structures of open and closed forms of binary and ternary complexes of the large fragment of Thermus aquaticus DNA polymerase I: structural basis for nucleotide incorporation, *Embo. J. 17*, 7514−7525.
6. Kunkel, T. A., and Bebenek, K. (2000) DNA replication fidelity, *Annu. Rev. Biochem. 69*, 497−529.
7. Bell, J. B., Eckert, K. A., Joyce, C. M., and Kunkel, T. A. (1997) Base miscoding and strand misalignment errors by mutator Klenow polymerases with amino acid substitutions at tyrosine 766 in the O helix of the fingers subdomain, *J. Biol. Chem. 272*, 7345−7351.
8. Carroll, S. S., Cowart, M., and Benkovic, S. J. (1991) A mutant of DNA polymerase I (Klenow fragment) with reduced fidelity, *Biochemistry 30*, 804−813.
9. Minnick, D. T., Bebenek, K., Osheroff, W. P., Turner, R. M., Jr., Astatke, M., Liu, L., Kunkel, T. A., and Joyce, C. M. (1999) Side chains that influence fidelity at the polymerase active site of Escherichia coli DNA polymerase I (Klenow fragment), *J. Biol. Chem. 274*, 3067−3075.
10. Astatke, M., Grindley, N. D., and Joyce, C. M. (1998) How E. coli DNA polymerase I (Klenow fragment) distinguishes between deoxy- and dideoxynucleotides, *J. Mol. Biol. 278*, 147−165.
11. Astatke, M., Ng, K., Grindley, N. D., and Joyce, C. M. (1998) A single side chain prevents Escherichia coli DNA polymerase I (Klenow fragment) from incorporating ribonucleotides, *Proc. Natl. Acad. Sci. U.S.A. 95*, 3402−3407.
12. Minnick, D. T., Liu, L., Grindley, N. D., Kunkel, T. A., and Joyce, C. M. (2002) Discrimination against purine-pyrimidine mispairs in the polymerase active site of DNA polymerase I: a structural explanation, *Proc. Natl. Acad. Sci. U.S.A. 99*, 1194−1199.
13. Dutta, S., Li, Y., Johnson, D., Dzantiev, L., Richardson, C. C., Romano, L. J., and Ellenberger, T. (2004) Crystal structures of 2-acetylaminofluorene and 2-aminofluorene in complex with T7 DNA polymerase reveal mechanisms of mutagenesis, *Proc. Natl. Acad. Sci. U.S.A. 101*, 16186−16191.
14. Hsu, G. W., Kiefer, J. R., Burnouf, D., Becherel, O. J., Fuchs, R. P., and Beese, L. S. (2004) Observing translesion synthesis of an aromatic amine DNA adduct by a high-fidelity DNA polymerase, *J. Biol. Chem. 279*, 50280−50285.
15. Beland, F. A., and Kadlubar, F. F. (1985) Formation and persistence of arylamine DNA adducts in vivo, *Environ. Health Perspect. 62*, 19−30.
16. Belguise-Valladier, P., and Fuchs, R. P. P. (1991) Strong sequence-dependent polymorphism in adduct-induced DNA structure: analysis of single N-2-acetylaminofluorene residues bound within the Nar I mutation hot spot, *Biochemistry 30*, 10091−10100.
17. Hingerty, B. E., and Broyde, S. (1986), *J. Biomol. Struct. Dyn. 4*, 365−372.
18. Mao, B., Hingerty, B. E., Broyde, S., and Patel, D. J. (1998) Solution structure of the aminofluorene [AF]-external conformer of the anti-[AF]-C8-dG adduct opposite dC in a DNA duplex, *Biochemistry 37*, 95−106.
19. O'Handley, S. F., Sanford, D. G., Xu, R., Lester, C. C., Hingerty, B. E., Broyde, S., and Krugh, T. R. (1993) Structural characterization of an N-acetyl-2-aminofluorene (AAF) modified DNA oligomer by NMR, energy minimization, and molecular dynamics, *Biochemistry 32*, 2481−2497.
20. Patel, D. J., Mao, B., Gu, Z., Hingerty, B. E., Gorin, A., Basu, A. K., and Broyde, S. (1998) Nuclear magnetic resonance solution structures of covalent aromatic amine-DNA adducts and their mutagenic relevance, *Chem. Res. Toxicol. 11*, 391−407.
21. van Houte, L. P. A., Bokma, J. T., Lutgerink, J. T., Westra, J. G., Retel, J., and van Grondelle, R. (1987) An optical study of the configuration of the aminofluorene-DNA complex, *Carcinogenesis 8*, 759−766.
22. Bichara, M., and Fuchs, R. P. P. (1985) DNA binding and mutation spectra of the carcinogen N-2-aminofluorene in Escherichia coli. A correlation between the conformation of the premutagenic lesion and the mutation specificity, *J. Mol. Biol. 183*, 341−351.
23. Hoffmann, G. R., and Fuchs, R. P. (1997) Mechanisms of frameshift mutations: insight from aromatic amines, *Chem. Res. Toxicol. 10*, 347−359.
24. Koffel-Schwartz, N., Verdier, J. M., Bichara, M., Freund, A. M., Daune, M. P., and Fuchs, R. P. (1984) Carcinogen-induced mutation spectrum in wild-type, uvrA and umuC strains of Escherichia coli. Strain specificity and mutation-prone sequences, *J. Mol. Biol. 177*, 33−51.
25. Lone, S., and Romano, L. J. (2003) Mechanistic insights into replication across from bulky DNA adducts: a mutant polymerase I allows an N-acetyl-2-aminofluorene adduct to be accommodated during DNA synthesis, *Biochemistry 42*, 3826−3834.
26. Joyce, C. M., and Derbyshire, V. (1995) Purification of Escherichia coli DNA polymerase I and Klenow fragment, *Methods Enzymol. 262*, 3−13.
27. Setlow, P. (1974) DNA polymerase I from Escherichia coli, *Methods Enzymol. 29*, 3−12.
28. Bradford, M. M. (1976) A rapid and sensitive method for the quantitation of microgram quantities of protein utilizing the principle of protein-dye binding, *Anal. Biochem. 72*, 248−254.

29. Dzantiev, L., and Romano, L. J. (1999) Interaction of Escherichia coli DNA polymerase I (Klenow fragment) with primer-templates containing N-acetyl-2-aminofluorene or N-2- aminofluorene adducts in the active site, *J. Biol. Chem. 274*, 3279−3284.
30. Shibutani, S., and Grollman, A. P. (1993) Nucleotide misincorporation on DNA templates containing N- (deoxyguanosin-N2-yl)-2-(acetylamino)fluorene, *Chem. Res. Toxicol. 6*, 819−824.
31. Alekseyev, Y. O., and Romano, L. J. (2000) In vitro replication of primer-templates containing benzo[a]pyrene adducts by exonuclease-deficient Escherichia coli DNA polymerase I (Klenow fragment): effect of sequence context on lesion bypass, *Biochemistry 39*, 10431−10438.
32. Mendelman, L. V., Boosalis, M. S., Petruska, J., and Goodman, M. F. (1989) Nearest neighbor influences on DNA polymerase insertion fidelity, *J. Biol. Chem. 264*, 14415−14423.
33. Mendelman, L. V., Petruska, J., and Goodman, M. F. (1990) Base mispair extension kinetics. Comparison of DNA polymerase alpha and reverse transcriptase, *J. Biol. Chem. 265*, 2338−2346.
34. Heflich, R. H., and Neft, R. E. (1994) Genetic toxicity of 2-acetylaminofluorene, 2-aminofluorene and some of their metabolites and model metabolites, *Mutat. Res. 318*, 73−114.
35. Doisy, R., and Tang, M. S. (1995) Effect of aminofluorene and (acetylamino)fluorene adducts on the DNA replication mediated by Escherichia coli polymerases I (Klenow fragment) and III, *Biochemistry 34*, 4358−4368.
36. Shibutani, S., Naomi, S., and Grollman, A. P. (1998) Mutagenic Specificity of (Acetylamino)fluorene-Derived DNA Adducts in Mammalian Cells, *Biochemistry 37*, 12034−12041.
37. Gill, J. P., and Romano, L. J. (2005) Mechanism for N-acetyl-2-aminofluorene-induced frameshift mutagenesis by Escherichia coli DNA polymerase I (Klenow fragment), *Biochemistry 44*, 15387−15395.
38. Shibutani, S., and Grollman, A. P. (1997) Molecular mechanisms of mutagenesis by aromatic amines and amides, *Mutat. Res. 376*, 71−78.
39. Minnick, D. T., Astatke, M., Joyce, C. M., and Kunkel, T. A. (1996) A thumb subdomain mutant of the large fragment of Escherichia coli DNA polymerase I with reduced DNA binding affinity, processivity, and frameshift fidelity, *J. Biol. Chem. 271*, 24954−24961.
40. Joyce, C. M., and Steitz, T. A. (1994) Function and structure relationships in DNA polymerases, *Annu. Rev. Biochem. 63*, 777−822.
41. Li, Y., Kong, Y., Korolev, S., and Waksman, G. (1998) Crystal structures of the Klenow fragment of Thermus aquaticus DNA polymerase I complexed with deoxyribonucleoside triphosphates, *Protein Sci. 7*, 1116−1123.
42. Ling, H., Boudsocq, F., Plosky, B. S., Woodgate, R., and Yang, W. (2003) Replication of a cis-syn thymine dimer at atomic resolution, *Nature 424*, 1083−1087.
43. Ling, H., Boudsocq, F., Woodgate, R., and Yang, W. (2001) Crystal structure of a Y-family DNA polymerase in action: a mechanism for error-prone and lesion-bypass replication, *Cell 107*, 91−102.
44. Ling, H., Boudsocq, F., Woodgate, R., and Yang, W. (2004) Snapshots of replication through an abasic lesion; structural basis for base substitutions and frameshifts, *Mol. Cell 13*, 751−762.
45. Ling, H., Sayer, J. M., Plosky, B. S., Yagi, H., Boudsocq, F., Woodgate, R., Jerina, D. M., and Yang, W. (2004) Crystal structure of a benzo[a]pyrene diol epoxide adduct in a ternary complex with a DNA polymerase, *Proc. Natl. Acad. Sci. U.S.A. 101*, 2265−2269.
46. Bresson, A., and Fuchs, R. P. (2002) Lesion bypass in yeast cells: Pol eta participates in a multi-DNA polymerase process, *EMBO J. 21*, 3881−3887.
47. Nelson, J. R., Gibbs, P. E., Nowicka, A. M., Hinkle, D. C., and Lawrence, C. W. (2000) Evidence for a second function for Saccharomyces cerevisiae Rev1p, *Mol. Microbiol. 37*, 549−554.
48. Prakash, S., and Prakash, L. (2002) Translesion DNA synthesis in eukaryotes: a one- or two-polymerase affair, *Genes Dev. 16*, 1872−1883.
49. Woodgate, R. (2001) Evolution of the two-step model for UV-mutagenesis, *Mutat. Res. 485*, 83−92.
50. Yang, W. (2003) Damage repair DNA polymerases Y, *Curr. Opin. Struct. Biol. 13*, 23−30.
51. Haracska, L., Washington, M. T., Prakash, S., and Prakash, L. (2001) Inefficient bypass of an abasic site by DNA polymerase eta, *J. Biol. Chem. 276*, 6861−6866.
52. Johnson, R. E., Washington, M. T., Haracska, L., Prakash, S., and Prakash, L. (2000) Eukaryotic polymerases iota and zeta act sequentially to bypass DNA lesions, *Nature 406*, 1015−1019.

BI061324O